$\mathrm{Mn_2}$ bis(pentalene): a mixed-spin bimetallic with two extremes of bonding within the same molecule†

Gabor Balazs,[a] F. Geoffrey N. Cloke,*[b] Andrew Harrison,[c] Peter B. Hitchcock,[b] Jennifer Green*[a] and Owen T. Summerscales[b]

Received (in Cambridge, UK) 10th October 2006, Accepted 9th November 2006
First published as an Advance Article on the web 1st December 2006
DOI: 10.1039/b614765h

Structural, magnetic and theoretical studies show that the bimetallic pentalene complex, $\mathrm{Mn_2(C_8H_4{}^{1,4\text{-}Si^iPr_3})_2}$, contains both high and low spin Mn(II) in two very different sites.

Manganese(II) is often shown to be atypical of the first row series, owing to the extra stabilisation energy of the unpaired high-spin d^5 configuration. In organometallic compounds variable multihaptic bonding of cyclopentadienyl is well known, a feature illustrated most effectively by manganocene $\mathrm{Mn(C_5H_5)_2}$.[1] It is unique as the only high-spin metallocene, causing myriad phenomena, as it forms conducting solutions in THF, undergoes facile ligand exchange, and is found in multiple forms in solid and solution states.[2–5] Molecular manganocene displays a partial spin-crossover at low temperatures, and further work substituting the rings with bulky or electron-donating substituents has created a whole series of both partial and complete spin-crossover compounds.[6–9] $\mathrm{Mn(C_5Me_5)_2}$ is a low-spin metallocene, with shorter Mn–C bonds, lower reactivity and no observed ligand exchange.[10,11] Recent work has also explored the supramolecular chemistry of the $\mathrm{[Mn(C_5H_5)_3]^-}$ anion.[12,13]

Metallocene-type environments may also be created using the eight-membered carbocyclic ligand pentalene $\mathrm{[C_8H_6]^{2-}}$, which may be commonly considered to act structurally as two fused cyclopentadienyl rings.[14] Katz *et al.* first synthesised the $\mathrm{M_2}$bis(pentalene) dimers for M = Co and Ni, in which twin metallocene-type environments were proposed.[14–16] Further work has extended this class of compounds to Mo, Rh and Pd centres using a triisopropylsilyl substituted pentalene, in which η^5:η^5-ligation is found in the crystal structures.[17–20]

It is clear that the manganocene and $\mathrm{M_2}$bis(pentalene) systems both present striking structural and electronic phenomena, which may lead, for example, to the development of novel magnetic materials. Therefore we have synthesised $\mathrm{Mn_2(C_8H_4{}^{1,4\text{-}Si^iPr_3})_2}$ and subsequently investigated its magnetic and structural properties. Reaction of an equimolar quantity of $\mathrm{C_8H_4{}^{1,4\text{-}Si^iPr_3}[K]_2}$ with $\mathrm{MnCl_2}$ in THF gives the bimetallic $\mathrm{Mn_2(C_8H_4{}^{1,4\text{-}Si^iPr_3})_2}$ (**1**) as a dark maroon, air-sensitive crystalline solid in 24% yield after workup (eqn (1)).‡

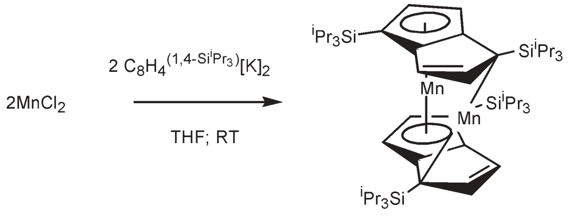

(1)

1

A single-crystal X-ray diffraction study reveals an asymmetric coordination environment in the molecule, with two distinctly different manganese centres bound to the ligands in different modes (Fig. 1).§ The structure also lies on a twofold rotation axis through a plane between the opposing pentalene ligands and bisecting the metal centres. Mn–C distances are given in Table 1. One $\mathrm{Mn^{II}}$ centre may be considered to be bound in an η^5:η^5-fashion, with a slighter shorter Mn–C(wingtip) distance (Mn1–C2) than the corresponding bridgehead distances (Mn1–C4, Mn1–C5). The other metal centre is however found significantly closer to the carbon with silyl substituents (Mn2–C8) than the remaining carbon atoms C4–C7 (the next closest is Mn2–C7). Consequent examination of C–C distances in the pentalene skeleton reveals a shorter bond between ring carbons C6–C7 of 1.383(7) Å, compared with an average of 1.444(7) Å for other C–C ring distances, consistent with a localised double bond.[19] The two ligands are slightly tilted away from each other (11°) and significantly twisted from an eclipsed conformation by 24° compared with 10° in $\mathrm{Mo_2(\eta^5{:}\eta^5\text{-}C_8H_4{}^{1,4\text{-}Si^iPr_3})_2}$.[17] A disproportionately large displacement ellipsoid for the Mn2 centre is observed, suggestive of a static or dynamic disorder between spatial positions of the metal cation. The Mn(1)···Mn(2) distance of 2.609(2) Å

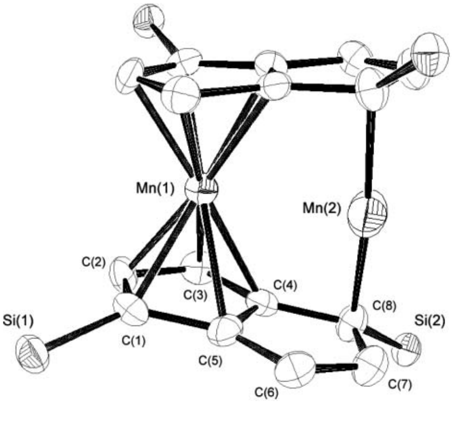

Fig. 1 Crystal structure of **1** (H and ^{i}Pr groups removed for clarity).

---

[a] *Department of Chemistry, University of Oxford, Inorganic Chemistry Laboratory, South Parks Road, UK, Oxford, OX1 3QR. E-mail: jennifer.green@chem.ox.ac.uk*
[b] *The Department of Chemistry, School of Life Sciences, University of Sussex, Brighton, UK BN1 9QJ. E-mail: f.g.cloke@sussex.ac.uk*
[c] *School of Chemistry, University of Edinburgh, Edinburgh, UK EH9 3JJ*

† The HTML version of this article has been enhanced with colour images.

Table 1 Experimental (Exptl.) and calculated (Calc.) Mn–C distances (Å) and atom–atom overlap populations (OP) for $Mn_2(C_8H_4R_2)_2$

	Mn1–C1	Mn1–C2	Mn1–C3	Mn1–C4	Mn1–C5	Mn2–C4	Mn2–C5	Mn2–C6	Mn2–C7	Mn2–C8
Exptl.	2.096(5)	2.085(5)	2.225(5)	2.194(5)	2.225(5)	2.471	2.804	2.692	2.313(5)	2.154(5)
Calc. (R = H)	2.10	2.07	2.13	2.15	2.18	2.62	2.78	2.57	2.28	2.25
Calc. (R = Si^iPr_3)	2.13	2.15	2.18	2.27	2.25	2.52	2.85	2.79	2.42	2.14
OP (R = H)	0.105	0.054	0.124	0.066	0.058	0.030	−0.013	0.031	0.118	0.155

may be considered short enough to constitute a formal metal–metal bond (which has been recently described between Mn^{II} centres at an internuclear distance of *ca.* 2.7–2.8 Å[21]) and this possibility is discussed following analysis of magnetic data and within a DFT study.

The complex is found to be highly paramagnetic, to the extent that it could not be characterised by NMR methods. Variable-temperature magnetic measurements in solution (Evans method, d_8-toluene) show that **1** does not obey the Curie–Weiss law; values of effective moment per dimer vary from 7.75 μ_B at 183 K, and decrease to 6.40 μ_B as the temperature was raised to 363 K (Fig. 2(a)). Data obtained for the solid-state susceptibilities (SQUID) meanwhile gave a lower moment of 5.15 μ_B at 4 K increasing slightly to 5.32 μ_B at 300 K (Fig. 2(b)). Fitting these values to a simple Curie–Weiss relationship gave a Curie constant of $C = 3.40$ emu K mol^{-1} and a Weiss constant of $\theta = -0.090$ K, showing essentially no additional coupling within the ground state. These values are consistent with an equilibrium between states with $S = 2$ and 3, the ground state differing between the solid state ($S = 2$; $\mu_{\text{spin-only}} = 4.90$ μ_B) and solution ($S = 3$; $\mu_{\text{spin-only}} = 6.92$ μ_B). In the latter case the ground state ($S = 3$) appears to be thermally depopulated into a state of lower spin multiplicity ($S = 2$) at higher temperatures.

In order to gain further insight into the bonding and spin-states of this unusual bimetallic, a DFT study was carried out on the model complex $[Mn_2(C_8H_6)_2]$ (**2**) using the hybrid B3LYP functional.¶ Comparing the relative energies of different spin-states of **2** shows that the septet ($S = 3$) spin-state is the lowest in energy but the quintet spin-state ($S = 2$) lies only 4.7 kJ mol^{-1} higher. The low energy difference between the septet ($S = 3$) and the quintet ($S = 2$) spin-states explain the variation of the magnetic moment of **1** in solution upon variation of the temperature. The triplet ($S = 1$) and the singlet ($S = 0$) spin-state are 135.3 and 244.9 kJ mol^{-1}, respectively, higher in energy whereas the nonet ($S = 4$) spin-state is 27.3 kJ mol^{-1} higher in energy than the septet spin-state.

Geometry optimization of **2** in the septet spin-state also reproduces best the geometric parameters of **1** (Table 1). However, the optimization in a quintet state gave a very similar structure. The asymmetric coordination of the pentalene units to the two different manganese atoms is retained. However, the ring 'slipping' in the optimized geometry of **2** is less accentuated than in the experimental structure of **1**. A QM/MM calculation on **1** with the Si^iPr_3 groups in the MM region gave a better agreement with experiment (Table 1), thus we attribute part of the twist to steric factors. The preferred binding of Mn2 to C8 is not only evident in the short distance but also the high value between these two atoms in the overlap population matrix (Table 1). This also indicates significant bonding between Mn2 and C7. The long distance between Mn2 and C6 is attributed to the single occupancy of the highest α spin orbital (Fig. 3) which shows a strong antibonding

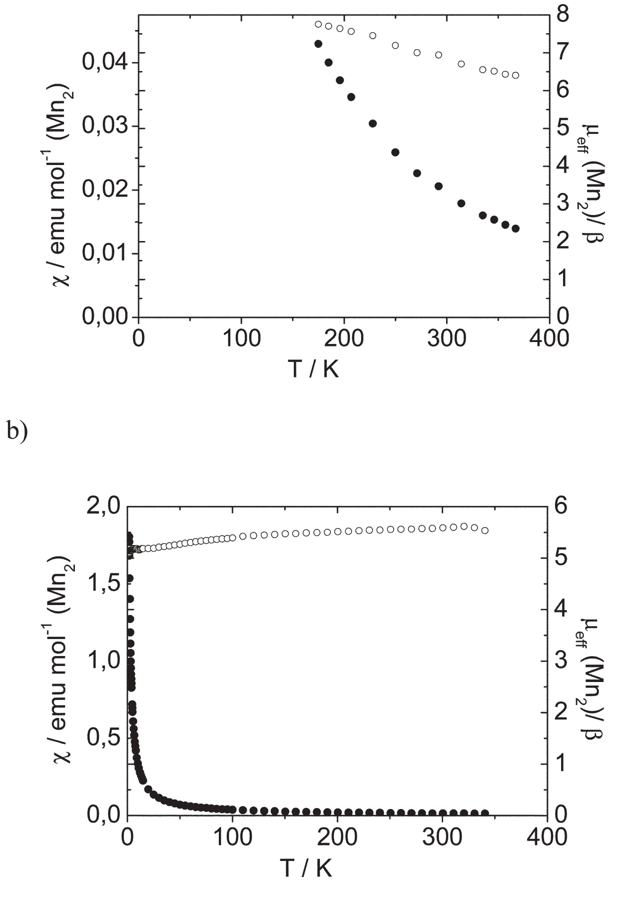

Fig. 2 Plot of molar susceptibility and effective magnetic moment for **1** measured using (a) the Evans' method and (b) a SQUID.

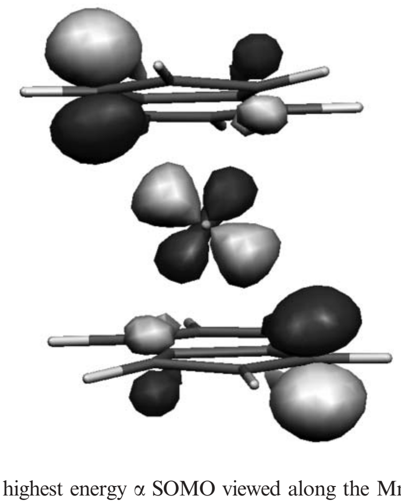

Fig. 3 The highest energy α SOMO viewed along the Mn–Mn C_2 axis.

interaction between this pair of atoms. The calculated Mn–Mn distance in **2** is slightly longer (2.69 Å) than in the experimental structure of **1** (2.609(2) Å).

An analysis of the atomic spin densities in the septet spin-state (S = 3) for both manganese atoms shows, that *ca.* 1.5 unpaired electrons are localised on Mn1 whereas on Mn2 there are 4.5 unpaired electrons. Almost the same atomic spin density distribution was found in the quintet (S = 2) spin-state, however in this spin-state antiferromagnetic coupling between the two Mn is observed.

To quantify the interaction between the two manganese atoms the Mn–Mn fractional bond order was calculated, by analyzing the interaction of a Mn_2 dimer with the two pentalene units.|| Considering the Mn_2 fragment σ_g, π_u and δ_g orbitals as bonding and σ_u, π_g and δ_u as antibonding and summing up the orbital populations in the complex a fractional bond order of 0.60 can be calculated. This suggests only a weak interaction between the two manganese centres.

Overall DFT suggests that **2** can best be described as having a S = 3 ground state containing a high spin as well as a low spin manganese.

In conclusion, $Mn_2(C_8H_4{}^{1,4\text{-Si}^i\text{Pr}_3})_2$ has two weakly interacting Mn(II) centres, one high spin and one low-spin, in different coordination environments. The low spin centre shows typical metallocene coordination whereas the high spin centre has a lower coordination number. This contrast strongly with the Mo analogue which is symmetric and shows strong Mo–Mo bonding.

Notes and references

‡ All procedures were carried out under Ar using standard Schlenk techniques in dry solvents. A THF solution of $C_8H_4{}^{1,4\text{-Si}^i\text{Pr}_3}[K]_2$ (246 mg, 0.5 mmol) was added dropwise to a suspension of $MnCl_2$ (63 mg, 0.5 mmol) in THF. A dark red solution resulted after 24 h of stirring, whereupon all volatiles were removed *in vacuo*. The dark residue was extracted with toluene (2 × 40 ml) and filtered through Celite to give a dark maroon red solution. The solution was concentrated (30 ml) and cooling to −50 °C overnight gave the product as dark red crystals. Yield: 110 mg (0.12 mmol, 24% yield). Anal. Calc. for $C_{52}H_{92}Si_4Mn_2$: C, 66.48; H, 9.87. Found: C, 66.52; H, 9.76%. MS (EI): m/z = 938 (100%, M^+); 884 (10%, $M^+ - Mn$).

§ *Crystal data* for **1**: M = 939.50, monoclinic, space group $C2/c$ (no. 15), a = 20.5816(9), b = 20.9291(11), c = 12.3807(4) Å, β = 94.419(3)°, V = 5317.2(4) $Å^3$, D_c = 1.17 Mg m^{-3}, T = 173(2) K, λ(Mo-Kα) = 0.71073 Å, Z = 4, μ = 0.60 mm^{-1}, $F(000)$ = 2040, crystal size 0.15 × 0.10 × 0.05 mm^3, θ range for data collection: 3.43–22.97°, index ranges hkl: −22 to 22, −22 to 22, −13 to 13, reflections collected = 29 478, independent reflections = 3668 (R_{int} = 0.103), reflections with $I > 2\sigma(I)$ = 2766, completeness to θ = 22.97° (99.3%), $T_{max, min}$ = 0.960 and 0.833, refinement method: full-matrix least squares on F^2, data/restraints/parameters = 3668/0/263, goodness-of-fit on F^2 = 1.105, final R indices [$I > 2\sigma(I)$] $R1$ = 0.067, $wR2$ = 0.151, R indices (all data): $R1$ = 0.098, $wR2$ = 0.165, Largest diff. peak and hole: 0.84 and −0.65 e $Å^{-3}$. The molecule lies on a twofold rotation axis. Data collection KappaCCD, program package WinGX, absorption correction MULTISCAN. Refinement using SHELXL-97. CCDC 623568. For crystallographic data in CIF or other electronic format see DOI: 10.1039/b614765h

¶ *Computational*: The geometries were optimized with the GAUSSIAN program using the B3LYP functional and the 6-31++G* basis sets for all atoms. For the comparison of the different spin-state energies of **2** the SCF energies were used.[22]

|| *Fragment calculations*: The fragment calculations were performed with the Amsterdam Density Functional (ADF) program package using the BP86 functional and TZP basis sets for all atoms.[23] In the fragment calculations the molecular orbitals of the molecule is constructed as a linear combination of the orbitals of the chosen fragments. The fragments retain the geometry they have in the whole molecule and are in a restricted spin states due to prior restricted calculations.

1 G. Wilkinson, F. A. Cotton and J. M. Birmingham, *J. Inorg. Nucl. Chem.*, 1956, **2**, 95–113.

2 M. E. Switzer and M. F. Rettig, *J. Chem. Soc., Chem. Commun.*, 1972, 687–688.

3 J. H. Ammeter, R. Bucher and N. J. Oswald, *J. Am. Chem. Soc.*, 1974, **96**, 7833–7835.

4 W. Bunder and E. Weiss, *Z. Naturforsch., Teil B*, 1978, **33**, 1235–1237.

5 F. H. Kohler and B. Schlesinger, *Inorg. Chem.*, 1992, **31**, 2853–2859.

6 S. Evans, M. L. H. Green, B. Jewitt, G. H. King and A. F. Orchard, *J. Chem. Soc., Faraday Trans. 2*, 1974, **70**, 356–376.

7 M. E. Switzer, R. Wang, M. F. Rettig and A. H. Maki, *J. Am. Chem. Soc.*, 1974, **96**, 7669–7674.

8 N. Hebendanz, F. H. Kohler, G. Muller and J. Riede, *J. Am. Chem. Soc.*, 1986, **108**, 3281–3289.

9 M. L. Hays, D. J. Burkey, J. S. Overby, T. P. Hanusa, S. P. Sellers, G. T. Yee and V. G. Young, *Organometallics*, 1998, **17**, 5521–5527.

10 J. C. Smart and J. L. Robbins, *J. Am. Chem. Soc.*, 1978, **100**, 3936–3937.

11 J. L. Robbins, N. M. Edelstein, S. R. Cooper and J. C. Smart, *J. Am. Chem. Soc.*, 1979, **101**, 3853–3857.

12 A. D. Bond, R. A. Layfield, J. A. MacAllister, M. McPartlin, J. M. Rawson and D. S. Wright, *Chem. Commun.*, 2001, 1956–1957.

13 S. Kheradmandan, H. W. Schmalle, H. Jacobsen, O. Blacque, T. Fox, H. Berke, M. Gross and S. DeCurtins, *Chem.–Eur. J.*, 2002, **8**, 2526.

14 O. T. Summerscales and F. G. N. Cloke, *Coord. Chem. Rev.*, 2005, **250**, 1122–1140.

15 T. J. Katz, N. Acton and J. McGinnis, *J. Am. Chem. Soc.*, 1972, **94**, 6205–6206.

16 T. J. Katz and N. Acton, *J. Am. Chem. Soc.*, 1972, **94**, 3281–3282.

17 M. C. Kuchta, F. G. N. Cloke and P. B. Hitchcock, *Organometallics*, 1998, **17**, 1934–1936.

18 C. Rivers, F. G. N. Cloke and P. B. Hitchcock, in preparation.

19 F. G. N. Cloke, J. C. Green, C. N. Jardine and M. C. Kuchta, *Organometallics*, 1999, **18**, 1087–1090.

20 E. Molins, W. Maniukiewicz, C. Miravitles, M. Mas, J. M. Manriquez, I. Chavez, B. Oelckers, J. Farran and J. L. Brianso, *Acta. Crystallogr., Sect. C*, 1996, **52**, 2414–2416.

21 S. Kheradmandan, T. Fox, H. W. Schmalle, K. Venkatesan and H. Berke, *Eur. J. Inorg. Chem.*, 2004, 3544–3554.

22 M. J. Frisch, G. W. Trucks, H. B. Schlegel, G. E. Scuseria, M. A. Robb, J. R. Cheeseman, J. A. Montgomery, Jr., T. Vreven, K. N. Kudin, J. C. Burant, J. M. Millam, S. S. Iyengar, J. Tomasi, V. Barone, B. Mennucci, M. Cossi, G. Scalmani, N. Rega, G. A. Petersson, H. Nakatsuji, M. Hada, M. Ehara, K. Toyota, R. Fukuda, J. Hasegawa, M. Ishida, T. Nakajima, Y. Honda, O. Kitao, H. Nakai, M. Klene, X. Li, J. E. Knox, H. P. Hratchian, J. B. Cross, V. Bakken, C. Adamo, J. Jaramillo, R. Gomperts, R. E. Stratmann, O. Yazyev, A. J. Austin, R. Cammi, C. Pomelli, J. Ochterski, P. Y. Ayala, K. Morokuma, G. A. Voth, P. Salvador, J. J. Dannenberg, V. G. Zakrzewski, S. Dapprich, A. D. Daniels, M. C. Strain, O. Farkas, D. K. Malick, A. D. Rabuck, K. Raghavachari, J. B. Foresman, J. V. Ortiz, Q. Cui, A. G. Baboul, S. Clifford, J. Cioslowski, B. B. Stefanov, G. Liu, A. Liashenko, P. Piskorz, I. Komaromi, R. L. Martin, D. J. Fox, T. Keith, M. A. Al-Laham, C. Y. Peng, A. Nanayakkara, M. Challacombe, P. M. W. Gill, B. G. Johnson, W. Chen, M. W. Wong, C. Gonzalez and J. A. Pople, *GAUSSIAN 03 (Revision C.02)*, Gaussian, Inc., Wallingford, CT, 2004.

23 *ADF2004.01*, SCM, Theoretical Chemistry, Vrije Universiteit, Amsterdam, The Netherlands, http://www.scm.com.